

Original citation:

LHCb Collaboration (Including Back, J. J., Blake, Thomas, Costa Sobral, Cayo, Crocombe, Andrew, Gershon, T. J., Kreps, Michal, Latham, Thomas, Loh, David, Mathad, Abhijit, O'Hanlon, Daniel P., Poluektov, Anton, Qian, W., Wallace, Charlotte and Wicht, Jean) (2017) Measurement of the CP violation parameter A_{Γ} in $D^0 \rightarrow K^+ K^-$ and $D^0 \rightarrow \pi^+ \pi^-$ decays. Physical Review Letters, 118 (26). 261803.

doi:10.1103/PhysRevLett.118.261803

Permanent WRAP URL:

<http://wrap.warwick.ac.uk/90426>

Copyright and reuse:

The Warwick Research Archive Portal (WRAP) makes this work of researchers of the University of Warwick available open access under the following conditions.

This article is made available under the Creative Commons Attribution 4.0 International license (CC BY 4.0) and may be reused according to the conditions of the license. For more details see: <http://creativecommons.org/licenses/by/4.0/>

A note on versions:

The version presented in WRAP is the published version, or, version of record, and may be cited as it appears here.

For more information, please contact the WRAP Team at: wrap@warwick.ac.uk

Measurement of the CP Violation Parameter A_Γ in $D^0 \rightarrow K^+K^-$ and $D^0 \rightarrow \pi^+\pi^-$ Decays

R. Aaij *et al.**

(LHCb Collaboration)

(Received 22 February 2017; published 28 June 2017)

Asymmetries in the time-dependent rates of $D^0 \rightarrow K^+K^-$ and $D^0 \rightarrow \pi^+\pi^-$ decays are measured in a pp collision data sample collected with the LHCb detector during LHC Run 1, corresponding to an integrated luminosity of 3 fb^{-1} . The asymmetries in effective decay widths between D^0 and \bar{D}^0 decays, sensitive to indirect CP violation, are measured to be $A_\Gamma(K^+K^-) = (-0.30 \pm 0.32 \pm 0.10) \times 10^{-3}$ and $A_\Gamma(\pi^+\pi^-) = (0.46 \pm 0.58 \pm 0.12) \times 10^{-3}$, where the first uncertainty is statistical and the second systematic. These measurements show no evidence for CP violation and improve on the precision of the previous best measurements by nearly a factor of two.

DOI: 10.1103/PhysRevLett.118.261803

Symmetry under the combined operations of charge conjugation and parity (CP) was found to be violated in flavor-changing interactions of the s quark [1], and later in processes involving the b quark [2,3]. Within the standard model, violation of CP symmetry in the charm sector is predicted at a level below $\mathcal{O}(10^{-3})$ [4,5]. Charm hadrons are the only particles where CP violation involving up-type quarks is expected to be observable, providing a unique opportunity to detect effects beyond the standard model that leave down-type quarks unaffected.

A sensitive probe of CP violation in the charm sector is given by decays of D^0 mesons into CP eigenstates f , where $f = \pi^+\pi^-$ or $f = K^+K^-$. The time-integrated CP asymmetries and the charm-mixing parameters $x \equiv (m_2 - m_1)/\Gamma$ and $y \equiv (\Gamma_2 - \Gamma_1)/(2\Gamma)$ [6], where $m_{1,2}$ and $\Gamma_{1,2}$ are the masses and widths of the mass eigenstates $|D_{1,2}\rangle$, are known to be small [7–9]. As a result, the time-dependent CP asymmetry of each decay mode can be approximated as [8]

$$A_{CP}(t) \equiv \frac{\Gamma(D^0(t) \rightarrow f) - \Gamma(\bar{D}^0(t) \rightarrow f)}{\Gamma(D^0(t) \rightarrow f) + \Gamma(\bar{D}^0(t) \rightarrow f)} \simeq a_{\text{dir}}^f - A_\Gamma \frac{t}{\tau_D}, \quad (1)$$

where $\Gamma(D^0(t) \rightarrow f)$ and $\Gamma(\bar{D}^0(t) \rightarrow f)$ indicate the time-dependent decay rates of an initial D^0 or \bar{D}^0 decaying to a final state f at decay time t , $\tau_D = 1/\Gamma = 2/(\Gamma_1 + \Gamma_2)$ is the average lifetime of the D^0 meson, a_{dir}^f is the asymmetry

related to direct CP violation, and A_Γ is the asymmetry between the D^0 and \bar{D}^0 effective decay widths

$$A_\Gamma \equiv \frac{\hat{\Gamma}_{D^0 \rightarrow f} - \hat{\Gamma}_{\bar{D}^0 \rightarrow f}}{\hat{\Gamma}_{D^0 \rightarrow f} + \hat{\Gamma}_{\bar{D}^0 \rightarrow f}}. \quad (2)$$

The effective decay width $\hat{\Gamma}_{D^0 \rightarrow f}$ is defined as $\int_0^\infty \Gamma(D^0(t) \rightarrow f) dt / \int_0^\infty t \Gamma(D^0(t) \rightarrow f) dt$, i.e., the inverse of the effective lifetime.

Neglecting contributions from subleading amplitudes [5,10], a_{dir}^f vanishes and A_Γ is independent of the final state f . Furthermore, in the absence of CP violation in mixing, it can be found that $A_\Gamma = -x \sin \phi$, where $\phi = \arg[(q\bar{A}_f)/(pA_f)]$, $A_f(\bar{A}_f)$ is the amplitude of the $D^0 \rightarrow f$ ($\bar{D}^0 \rightarrow f$) decay, and p and q are the coefficients of the decomposition of the mass eigenstates $|D_{1,2}\rangle = p|D^0\rangle \pm q|\bar{D}^0\rangle$. This implies that $|A_\Gamma| < |x| \lesssim 5 \times 10^{-3}$ [6].

This Letter presents a measurement of A_Γ with pp collision data collected by LHCb in Run 1, corresponding to an integrated luminosity of 3 fb^{-1} , with 1 fb^{-1} collected during 2011 at a center-of-mass energy of 7 TeV and 2 fb^{-1} collected during 2012 at 8 TeV. The measurements presented are independent of the center-of-mass energy, but the two periods are analyzed separately to account for differences in cross sections and in the general running conditions. The charge of the pion from the $D^{*+} \rightarrow D^0\pi^+$ ($D^{*-} \rightarrow \bar{D}^0\pi^-$) decay is used to identify the flavor of the D^0 (\bar{D}^0) meson at production. Two different approaches are used to perform the measurement of A_Γ . The first is a new method based on Eq. (1) and provides the more precise results. This is described in the following text, unless otherwise stated. The other method, based on Eq. (2), has been described previously in Ref. [11] and is only summarized here. In the following, inclusion of charge-conjugate processes is implied throughout, unless otherwise stated.

*Full author list given at the end of the article.

Published by the American Physical Society under the terms of the Creative Commons Attribution 4.0 International license. Further distribution of this work must maintain attribution to the author(s) and the published article's title, journal citation, and DOI.

The LHCb detector [12,13] is a single-arm forward spectrometer covering the pseudorapidity range $2 < \eta < 5$, designed for the study of particles containing b or c quarks. The detector includes a high-precision tracking system consisting of a silicon-strip vertex detector, surrounding the pp interaction region and allowing c hadrons to be identified by their characteristic flight distance, a large-area silicon-strip detector located upstream of a dipole magnet with a bending power of about 4 Tm and three stations of silicon-strip detectors and straw drift tubes placed downstream of the magnet. Two ring-imaging Cherenkov detectors provide particle identification to distinguish kaons from pions. The polarity of the dipole magnet is periodically reversed during data taking. The configuration with the magnetic field vertically upwards (downwards), MagUp (MagDown), bends positively (negatively) charged particles in the horizontal plane towards the center of the Large Hadron Collider. The LHCb coordinate system is a right-handed system, with the z axis pointing along the beam direction, y pointing vertically upwards, and x pointing in the horizontal direction away from the collider center.

An online event selection is performed by a trigger system [14], consisting of a hardware stage, based on information from the calorimeter and muon systems, followed by a software stage, which applies a full event reconstruction. All events passing the hardware trigger are analyzed. Both the software trigger and the subsequent event selection use kinematic and topological variables to separate signal decays from the background. In the software trigger, two oppositely charged particles are required to form a D^0 candidate that is significantly displaced from any primary pp interaction vertex (PV) in the event, and at least one of these two particles must have a minimum momentum transverse to the beam direction of 1.7 GeV/ c or 1.6 GeV/ c , depending on the running conditions. The D^0 candidates are combined with all possible pion candidates (“soft pions”) to form D^{*+} candidates. No requirements are imposed on the soft pions at trigger level.

Offline requirements are placed on the D^{*+} vertex fit quality, where the vertex formed by the D^0 and the soft π^+ candidate is constrained to coincide with a PV, the D^0 flight distance and transverse momentum, the angle between the D^0 momentum and the vector from the PV to the D^0 decay vertex, and the χ_{IP}^2 value of each of the D^0 decay products, where χ_{IP}^2 is defined as the difference between the vertex fit χ^2 of a PV reconstructed with and without the particle under consideration. The two signal samples, $\pi^+\pi^-$ and K^+K^- , plus the Cabibbo-favored $K^-\pi^+$ control sample, are defined imposing further requirements on the particle identification likelihood, which is calculated from a combination of information from the Cherenkov detectors and the tracking system [15]. About 13% of the selected events have more than one candidate, mostly due to a single D^0 candidate being associated with multiple soft pions. One of those candidates is then selected at random.

The D^0 signal region is defined by the requirement that the invariant mass be within ± 24 MeV/ c^2 (approximately ± 3 times the mass resolution) of the known value [16]. The reconstructed decay times of charm mesons that originate from weak decays of b hadrons (secondary decays) are biased towards positive values, and thus, these decays are treated as background. This contamination is reduced to a few percent by requiring the reconstructed D^0 momentum to point back to the PV, and $\chi_{\text{IP}}^2(D^0) < 9$. A systematic uncertainty on the final measurement is assigned due to the residual secondary background. The signal yields of the K^+K^- , $\pi^+\pi^-$ and $K^-\pi^+$ samples, obtained by fitting the distributions of the invariant mass difference $\Delta m \equiv m(D^0\pi^+) - m(D^0)$, are reported in Table I. A Johnson S_U distribution [17] plus the sum of three Gaussian functions is used to model the signal, while the background is described by an empirical function of the form $1 - \exp[(\Delta m - \Delta m_0)/\alpha] + \beta(\Delta m/\Delta m_0 - 1)$, where Δm_0 is the threshold of the function, and α and β describe its shape.

The effect of a small residual background of fake D^{*+} candidates, dominated by real D^0 decays associated with uncorrelated pions, is removed by a sideband-subtraction procedure. The signal region is defined as $\Delta m \in [144.45, 146.45]$ MeV/ c^2 , about ± 5 times the Δm resolution, and the sideband region as $\Delta m \in [149, 154]$ MeV/ c^2 . The uncertainty associated with this procedure is accounted for within the systematic uncertainty.

The structure of the LHCb detector is nearly symmetric under reflection in the vertical plane containing the beam axis. Nevertheless, departures from the nominal geometry and variations of the efficiency in different parts of the detector produce small residual deviations from an ideally symmetric detector acceptance. An important part of the analysis is therefore the determination and correction of these residual asymmetries. The method to achieve this is developed by exploiting the large control sample available in the $D^0 \rightarrow K^-\pi^+$ mode, where the time-dependent asymmetry is expected to be negligible. The distribution of the D^0 decay time in the range $[0.6\tau_D, 20\tau_D]$ is divided into 30 approximately equally populated bins, and the $D^0\text{-}\bar{D}^0$ yield asymmetry after background removal is determined in each of them. The lower bound is introduced to remove the initial turn-on region of the trigger efficiency

TABLE I. Signal yields in millions after all selection requirements.

Subsample	$D^0 \rightarrow K^-\pi^+$	$D^0 \rightarrow K^+K^-$	$D^0 \rightarrow \pi^+\pi^-$
2011 MagUp	10.7	1.2	0.4
2011 MagDown	15.5	1.7	0.5
2012 MagUp	30.0	3.3	1.0
2012 MagDown	31.3	3.4	1.1
Total	87.5	9.6	3.0

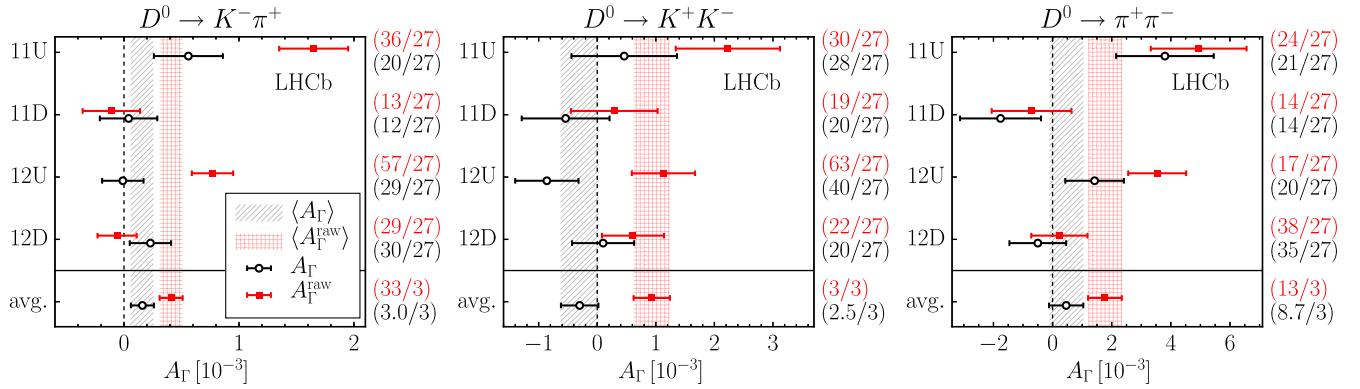


FIG. 1. Results from A_T fits in each subsample before (solid red squares) and after (empty black dots) the asymmetry correction. Fit qualities ($\chi^2/\text{number of degrees of freedom}$) are also reported to the right of each graph. The weighted average of the four A_T values is indicated before (red hatched band) and after (black hatched band) the correction. The numerical values for the averages are $A_T(K^-\pi^+) = (0.41 \pm 0.10) \times 10^{-3}$, $A_T(K^+K^-) = (0.93 \pm 0.31) \times 10^{-3}$, and $A_T(\pi^+\pi^-) = (1.77 \pm 0.57) \times 10^{-3}$ before the correction and $A_T(K^-\pi^+) = (0.16 \pm 0.10) \times 10^{-3}$, $A_T(K^+K^-) = (-0.30 \pm 0.32) \times 10^{-3}$, and $A_T(\pi^+\pi^-) = (0.46 \pm 0.58) \times 10^{-3}$ after the correction. The label 2011 (2012) is abbreviated 11 (12) and MagUp (MagDown) is abbreviated $U(D)$.

to avoid potential biases due to charge asymmetries of the quickly varying acceptance function. The measured asymmetry $A(t)$ is then fitted with a linear function of the decay time in units of τ_D , the slope of which is taken as the estimate of A_T [see Eq. (1)]. For the $\pi^+\pi^-$ and K^+K^- final states, the slope is kept blind until the completion of the analysis. The slope for the $K^-\pi^+$ sample, expected to be unmeasurably small, is not blinded. Figure 1 shows the values of A_T obtained in the four subsamples defined in Table I. The presence of significant deviations from zero for the control channel indicates the existence of non-negligible time-dependent residual detector asymmetries. They partially cancel in the combination of the MagUp and MagDown samples but not completely, yielding an overall average that is incompatible with zero. These residual biases arise due to correlations between the decay time and other kinematic variables that affect the efficiency, most notably the momentum of the soft pion.

A correction to remove the dependence of detection asymmetries on the soft pion kinematics is applied in the time-integrated $(k, q_s\theta_x, \theta_y)$ distribution, where $k = 1/\sqrt{p_x^2 + p_z^2}$ is proportional to the curvature of the trajectory in the magnetic field, q_s is the sign of the soft pion charge, and $\theta_x = \arctan(p_x/p_z)$ and $\theta_y = \arctan(p_y/p_z)$ are the pion emission angles in the bending and vertical planes, respectively. In the absence of any asymmetry in the sample or in the detector acceptance, this distribution should be identical for D^{*+} and D^{*-} decays. A statistically significant asymmetry is, however, observed in the $K^-\pi^+$ data (Fig. 2), where the most visible features are due to geometric boundaries of the detector, where the acceptance for positive and negative tracks differ. For each of the three decay modes, candidates are therefore weighted to fulfill $N^+(k, +\theta_x, \theta_y) = N^-(k, -\theta_x, \theta_y)$, where N^\pm is the number of reconstructed $D^{*\pm}$ decays in a given bin.

The granularity of the correction is finer in $(k, q_s\theta_x)$ than in θ_y , where only small nonuniformities are present [18].

The weighting procedure corrects for any asymmetry of the detector response but also removes any global asymmetry caused by either CP violation or differences in the production cross sections for D^{*+} and D^{*-} . Simulation studies have confirmed that this procedure, while canceling the time-integrated asymmetry, has no significant effect on a possible genuine time-dependent asymmetry. The asymmetry correction is independently determined and applied within each subsample; the convergence of all A_T values for the $K^-\pi^+$ control sample to a common value, as seen in Fig. 1 (top), thus provides a cross-check of the validity of the method. Independent application of the same asymmetry correction procedure to the $D^0 \rightarrow K^+K^-$ and $D^0 \rightarrow \pi^+\pi^-$ modes also leads to good quality for the decay-time fit in each subsample and good consistency among subsamples, as shown in Fig. 1 (bottom left and bottom right).

Another effect that needs to be accounted for in the measurement of A_T is the residual contamination from D^{*+} mesons produced in b -hadron decays. This contribution to the measured asymmetry is described with the expression

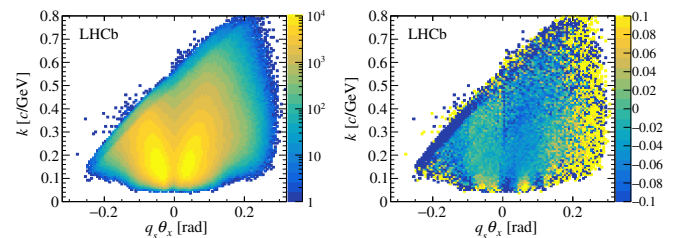


FIG. 2. (Left) Sum and (right) asymmetry of distributions of positive and negative soft pions in the $(k, q_s\theta_x)$ plane for the 2011 MagUp $D^0 \rightarrow K^-\pi^+$ subsample after integration over θ_y .

$$A(t) = (1 - f_{\text{sec}}(t))A_{\text{prompt}}(t) + f_{\text{sec}}(t)A_{\text{sec}}(t),$$

where $A_{\text{prompt}}(t)$ and $A_{\text{sec}}(t)$ are the asymmetries for prompt and secondary components, and $f_{\text{sec}}(t)$ is the fraction of secondary decays in the sample at decay time t . This fraction is estimated from a simulation-based model calibrated by the yield of secondary decays in data, obtained at high values of t from fits to the $\chi_{\text{IP}}^2(D^0)$ distribution, while $A_{\text{sec}}(t)$ is obtained from a data sample with $\ln(\chi_{\text{IP}}^2(D^0)) > 4$. From these estimates, the maximum effect of the contamination of secondary decays is assessed as $\delta A_{\Gamma}^{KK} = 0.08 \times 10^{-3}$ and $\delta A_{\Gamma}^{\pi\pi} = 0.12 \times 10^{-3}$, accounting for the uncertainty due to the determination of $A_{\text{sec}}(t)$ and $f_{\text{sec}}(t)$ and for the possible contribution of nonzero values of A_{Γ}^{KK} and $A_{\Gamma}^{\pi\pi}$ [18]. These effects are much smaller than the statistical uncertainties and are assigned as systematic uncertainties.

Many other effects have been examined as potential sources of systematic uncertainty. The uncertainty on the random pion background subtraction has been evaluated from the measured asymmetry of the background and its variation across the mass range surrounding the signal peak in the Δm distribution, yielding an uncertainty of $\delta A_{\Gamma} = 0.01 \times 10^{-3}$ for both modes. The effect of approximating the continuous three-dimensional $(k, q, \theta_x, \theta_y)$ asymmetry correction with a discrete function has been estimated by repeating the extraction of A_{Γ} in the $K^-\pi^+$ control sample with twice or half the number of bins, which leads to an uncertainty of 0.02×10^{-3} for both decay modes. An additional uncertainty in the K^+K^- mode due to the presence of a peaking background from real $D^{*+} \rightarrow D^0\pi^+$ decays, with the D^0 meson decaying into other final states, has been evaluated as $\delta A_{\Gamma}^{KK} = 0.05 \times 10^{-3}$, based on a study of the sidebands of the D^0 candidate mass distribution. Other possible sources of systematic uncertainty, including the resolution of the decay-time measurement, are found to be negligible.

The final results, obtained from the weighted average of the values separately extracted from time-dependent fits of each subsample (Fig. 1), are $A_{\Gamma}(K^+K^-) = (-0.30 \pm 0.32 \pm 0.10) \times 10^{-3}$ and $A_{\Gamma}(\pi^+\pi^-) = (0.46 \pm 0.58 \pm 0.12) \times 10^{-3}$, where the first uncertainty is statistical and the second is systematic. Time-dependent asymmetries averaged over the full Run 1 data sample are compared with fit results in Fig. 3.

The complementary analysis based on Eq. (2) follows a procedure largely unchanged from the previous LHCb analysis [11], described in Refs. [19,20] and briefly summarized below. The selection requirements for this method differ from those based on Eq. (1) only in the lack of a requirement on $\chi_{\text{IP}}^2(D^0)$. A similar blinding procedure is used. This analysis is applied to the 2 fb^{-1} subsample of the present data, collected in 2012, that was not used in Ref. [11]. The 2012 data are split into three data-taking

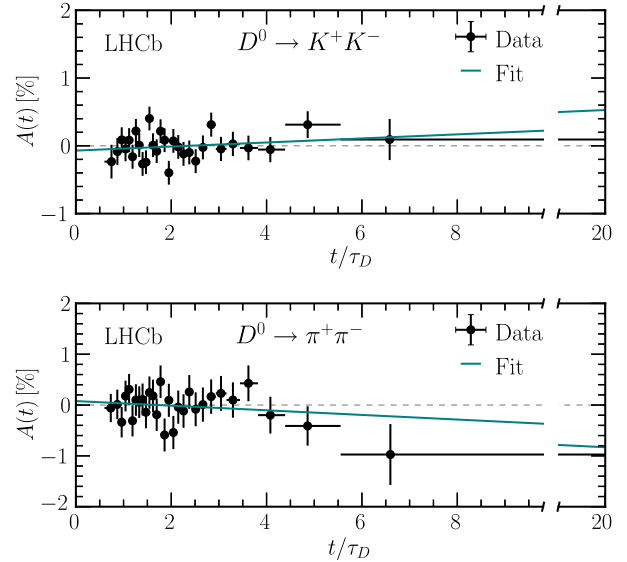


FIG. 3. Measured asymmetry $A(t)$ in bins of t/τ_D , where $\tau_D = 0.410 \text{ ps}$ [16] for (top) $D^0 \rightarrow K^+K^-$ and (bottom) $D^0 \rightarrow \pi^+\pi^-$, averaged over the full Run 1 data sample. Solid lines show the time dependence with a slope equal to the best estimates of $-A_{\Gamma}$.

periods to account for known differences in the detector alignment and calibration after detector interventions.

Biases on the decay-time distribution, introduced by the selection criteria and detection asymmetries, are accounted for through per-candidate acceptance functions, as described in Ref. [20]. These acceptance functions are parametrized by the decay-time intervals within which a candidate would pass the event selection if its decay time could be varied. They are determined using a data-driven method and used to normalize the per-candidate probability density functions over the decay-time range in which the candidate would be accepted.

A two-stage unbinned maximum likelihood fit is used to determine the effective decay widths. In the first stage, fits to the D^0 mass and Δm spectra are used to determine yields of signal decays and both combinatorial and partially reconstructed backgrounds. In the second stage, a fit to the decay-time distribution, together with $\ln(\chi_{\text{IP}}^2(D^0))$ (Fig. 4), is made to separate secondary background. The finding of an asymmetry consistent with zero in the control channel, $A_{\Gamma}(K^-\pi^+) = (-0.07 \pm 0.15) \times 10^{-3}$, validates the method. Small mismodeling effects are observed in the decay-time fits, and a corresponding systematic uncertainty of 0.04×10^{-3} (0.09×10^{-3}) for K^+K^- ($\pi^+\pi^-$) is assigned. The largest systematic uncertainty for the A_{Γ} measurement, with K^+K^- ($\pi^+\pi^-$), is 0.08×10^{-3} (0.10×10^{-3}) due to the uncertainty in modeling the contamination from the secondary (combinatorial) background. The results from the 2012 data sample are $A_{\Gamma}(K^+K^-, 2012) = (-0.03 \pm 0.46 \pm 0.10) \times 10^{-3}$ and $A_{\Gamma}(\pi^+\pi^-, 2012) = (0.03 \pm 0.79 \pm 0.16) \times 10^{-3}$. These results are then combined with results from Ref. [11]

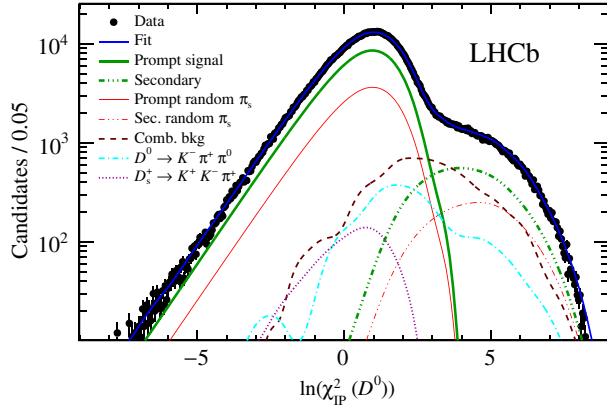


FIG. 4. Distribution of $\ln(\chi_{\text{IP}}^2(D^0))$ for the $D^0 \rightarrow K^+K^-$ candidates selected in the second of the three 2012 data-taking periods with magnetic field pointing downwards. The unbinned maximum likelihood fit results are overlaid. Gaussian kernels are used to smooth the combinatorial and partially reconstructed backgrounds.

to yield the final Run 1 measurements: $A_\Gamma(K^+K^-) = (-0.14 \pm 0.37 \pm 0.10) \times 10^{-3}$ and $A_\Gamma(\pi^+\pi^-) = (0.14 \pm 0.63 \pm 0.15) \times 10^{-3}$.

These results can be compared with the final results from the method based on Eq. (1). An analysis has been carried out to estimate the statistical correlation between the results from the two methods, with the conclusion that they agree within one standard deviation. Because of the large correlation, the measurements from the two methods are not combined, but rather, the more precise one is chosen as the nominal result.

The results for $D^0 \rightarrow K^+K^-$ and $D^0 \rightarrow \pi^+\pi^-$ are consistent and show no evidence of CP violation. Assuming that only indirect CP violation contributes to A_Γ [5] and accounting for correlations between the systematic uncertainties [21], the two values, obtained with the method using Eq. (1), can be averaged to yield a single value of $A_\Gamma = (-0.13 \pm 0.28 \pm 0.10) \times 10^{-3}$, while their difference is $\Delta A_\Gamma = (-0.76 \pm 0.66 \pm 0.04) \times 10^{-3}$. The above average is consistent with the result obtained by LHCb in a muon-tagged sample [22], which is statistically independent. The two results are therefore combined to yield an overall LHCb Run 1 value $A_\Gamma = (-0.29 \pm 0.28) \times 10^{-3}$ for the average of the K^+K^- and $\pi^+\pi^-$ modes. The measurements of A_Γ reported in this Letter are the most precise to date and are consistent with previous results [11,23,24]. They supersede the previous LHCb measurement [11] with an improvement in precision by nearly a factor of two.

We express our gratitude to our colleagues in the CERN accelerator departments for the excellent performance of the LHC. We thank the technical and administrative staff at the LHCb institutes. We acknowledge support from CERN and from the national agencies: CAPES, CNPq, FAPERJ and FINEP (Brazil); MOST and NSFC (China); CNRS/IN2P3

(France); BMBF, DFG and MPG (Germany); INFN (Italy); FOM and NWO (The Netherlands); MNiSW and NCN (Poland); MEN/IFA (Romania); MinES and FASO (Russia); MinECo (Spain); SNSF and SER (Switzerland); NASU (Ukraine); STFC (United Kingdom); NSF (USA). We acknowledge the computing resources that are provided by CERN, IN2P3 (France), KIT and DESY (Germany), INFN (Italy), SURF (The Netherlands), PIC (Spain), GridPP (United Kingdom), RRCKI and Yandex LLC (Russia), CSCS (Switzerland), IFIN-HH (Romania), CBPF (Brazil), PL-GRID (Poland), and OSC (USA). We are indebted to the communities behind the multiple open source software packages on which we depend. Individual groups or members have received support from AvH Foundation (Germany), EPLANET, Marie Skłodowska-Curie Actions and ERC (European Union), Conseil Général de Haute-Savoie, Labex ENIGMASS and OCEVU, Région Auvergne (France), RFBR and Yandex LLC (Russia), GVA, XuntaGal and GENCAT (Spain), Herchel Smith Fund, The Royal Society, Royal Commission for the Exhibition of 1851, and the Leverhulme Trust (United Kingdom).

-
- [1] J. H. Christenson, J. W. Cronin, V. L. Fitch, and R. Turlay, *Phys. Rev. Lett.* **13**, 138 (1964).
 - [2] B. Aubert *et al.* (BABAR collaboration), *Phys. Rev. Lett.* **87**, 091801 (2001).
 - [3] K. Abe *et al.* (Belle Collaboration), *Phys. Rev. Lett.* **87**, 091802 (2001).
 - [4] M. Bobrowski, A. Lenz, J. Riedl, and J. Rohrwild, *J. High Energy Phys.* **03** (2010) 009.
 - [5] Y. Grossman, A. L. Kagan, and Y. Nir, *Phys. Rev. D* **75**, 036008 (2007).
 - [6] Y. Amhis *et al.* (Heavy Flavor Averaging Group), [arXiv:1612.07233](https://arxiv.org/abs/1612.07233).
 - [7] R. Aaij *et al.* (LHCb Collaboration), *Phys. Rev. Lett.* **111**, 251801 (2013).
 - [8] T. Aaltonen *et al.* (CDF Collaboration), *Phys. Rev. D* **85**, 012009 (2012).
 - [9] R. Aaij *et al.* (LHCb Collaboration), *Phys. Lett. B* **767**, 177 (2017).
 - [10] D.-s. Du, *Eur. Phys. J. C* **50**, 579 (2007).
 - [11] R. Aaij *et al.* (LHCb Collaboration), *Phys. Rev. Lett.* **112**, 041801 (2014).
 - [12] A. A. Alves Jr. *et al.* (LHCb Collaboration), *JINST* **3**, S08005 (2008).
 - [13] R. Aaij *et al.* (LHCb Collaboration), *Int. J. Mod. Phys. A* **30**, 1530022 (2015).
 - [14] R. Aaij *et al.*, *JINST* **8**, P04022 (2013).
 - [15] M. Adinolfi *et al.*, *Eur. Phys. J. C* **73**, 2431 (2013).
 - [16] C. Patrignani *et al.* (Particle Data Group), *Chin. Phys. C* **40**, 100001 (2016).
 - [17] N. Johnson, *Biometrika* **36**, 149 (1949).
 - [18] P. Marino, Ph.D. thesis, Scuola Normale Superiore, 2017. CERN Report No. CERN-THESIS-2017-007, <https://cds.cern.ch/record/2248481>.

- [19] R. Aaij *et al.* (LHCb Collaboration), *J. High Energy Phys.* **04** (2012) 129.
- [20] V. V. Gligorov, R. Aaij, M. Cattaneo, M. Clemencic, M. Gersabeck, A. Falabella, E. Van Herwijnen, N. Torr, G. Raven, and F. Stagni, *J. Phys. Conf. Ser.* **396**, 022016 (2012).
- [21] R. Nisius, *Eur. Phys. J. C* **74**, 3004 (2014).
- [22] R. Aaij *et al.* (LHCb Collaboration), *J. High Energy Phys.* **04** (2015) 043.
- [23] J. P. Lees *et al.* (BABAR collaboration), *Phys. Rev. D* **87**, 012004 (2013).
- [24] T. A. Aaltonen *et al.* (CDF Collaboration), *Phys. Rev. D* **90**, 111103 (2014).

R. Aaij,⁴⁰ B. Adeva,³⁹ M. Adinolfi,⁴⁸ Z. Ajaltouni,⁵ S. Akar,⁵⁹ J. Albrecht,¹⁰ F. Alessio,⁴⁰ M. Alexander,⁵³ S. Ali,⁴³ G. Alkhazov,³¹ P. Alvarez Cartelle,⁵⁵ A. A. Alves Jr.,⁵⁹ S. Amato,² S. Amerio,²³ Y. Amhis,⁷ L. An,³ L. Anderlini,¹⁸ G. Andreassi,⁴¹ M. Andreotti,^{17,a} J. E. Andrews,⁶⁰ R. B. Appleby,⁵⁶ F. Archilli,⁴³ P. d'Argent,¹² J. Arnau Romeu,⁶ A. Artamonov,³⁷ M. Artuso,⁶¹ E. Aslanides,⁶ G. Auricemma,²⁶ M. Baalouch,⁵ I. Babuschkin,⁵⁶ S. Bachmann,¹² J. J. Back,⁵⁰ A. Badalov,³⁸ C. Baesso,⁶² S. Baker,⁵⁵ V. Balagura,^{7,b} W. Baldini,¹⁷ R. J. Barlow,⁵⁶ C. Barschel,⁴⁰ S. Barsuk,⁷ W. Barter,⁵⁶ F. Baryshnikov,³² M. Baszczyk,²⁷ V. Batozskaya,²⁹ B. Batsukh,⁶¹ V. Battista,⁴¹ A. Bay,⁴¹ L. Beaucourt,⁴ J. Beddow,⁵³ F. Bedeschi,²⁴ I. Bediaga,¹ A. Beiter,⁶¹ L. J. Bel,⁴³ V. Bellee,⁴¹ N. Belloli,^{21,c} K. Belous,³⁷ I. Belyaev,³² E. Ben-Haim,⁸ G. Bencivenni,¹⁹ S. Benson,⁴³ S. Beranek,⁹ A. Berezhnoy,³³ R. Bernet,⁴² A. Bertolin,²³ C. Betancourt,⁴² F. Betti,¹⁵ M.-O. Bettler,⁴⁰ M. van Beuzekom,⁴³ I. Bezshyiko,⁴² S. Bifani,⁴⁷ P. Billoir,⁸ T. Bird,⁵⁶ A. Birnkraut,¹⁰ A. Bitadze,⁵⁶ A. Bizzeti,^{18,d} T. Blake,⁵⁰ F. Blanc,⁴¹ J. Blouw,¹¹ S. Blusk,⁶¹ V. Bocci,²⁶ T. Boettcher,⁵⁸ A. Bondar,^{36,e} N. Bondar,^{31,40} W. Bonivento,¹⁶ I. Bordyuzhin,³² A. Borgheresi,^{21,c} S. Borghi,⁵⁶ M. Borisyak,³⁵ M. Borsato,³⁹ F. Bossu,⁷ M. Boubdir,⁹ T. J. V. Bowcock,⁵⁴ E. Bowen,⁴² C. Bozzi,^{17,40} S. Braun,¹² M. Britsch,¹² T. Britton,⁶¹ J. Brodzicka,⁵⁶ E. Buchanan,⁴⁸ C. Burr,⁵⁶ A. Bursche,² J. Buytaert,⁴⁰ S. Cadeddu,¹⁶ R. Calabrese,^{17,a} M. Calvi,^{21,c} M. Calvo Gomez,^{38,f} A. Camboni,³⁸ P. Campana,¹⁹ D. H. Campora Perez,⁴⁰ L. Capriotti,⁵⁶ A. Carbone,^{15,g} G. Carboni,^{25,h} R. Cardinale,^{20,i} A. Cardini,¹⁶ P. Carniti,^{21,c} L. Carson,⁵² K. Carvalho Akiba,² G. Casse,⁵⁴ L. Cassina,^{21,c} L. Castillo Garcia,⁴¹ M. Cattaneo,⁴⁰ G. Cavallero,²⁰ R. Cenci,^{24,j} D. Chamont,⁷ M. Charles,⁸ Ph. Charpentier,⁴⁰ G. Chatzikonstantinidis,⁴⁷ M. Chefdeville,⁴ S. Chen,⁵⁶ S.-F. Cheung,⁵⁷ V. Chobanova,³⁹ M. Chrzaszcz,^{42,27} X. Cid Vidal,³⁹ G. Ciezarek,⁴³ P. E. L. Clarke,⁵² M. Clemencic,⁴⁰ H. V. Cliff,⁴⁹ J. Closier,⁴⁰ V. Coco,⁵⁹ J. Cogan,⁶ E. Cogneras,⁵ V. Cogoni,^{16,40,k} L. Cojocariu,³⁰ P. Collins,⁴⁰ A. Comerma-Montells,¹² A. Contu,⁴⁰ A. Cook,⁴⁸ G. Coombs,⁴⁰ S. Coquereau,³⁸ G. Corti,⁴⁰ M. Corvo,^{17,a} C. M. Costa Sobral,⁵⁰ B. Couturier,⁴⁰ G. A. Cowan,⁵² D. C. Craik,⁵² A. Crocombe,⁵⁰ M. Cruz Torres,⁶² S. Cunliffe,⁵⁵ R. Currie,⁵⁵ C. D'Ambrosio,⁴⁰ F. Da Cunha Marinho,² E. Dall'Occo,⁴³ J. Dalseno,⁴⁸ P. N. Y. David,⁴³ A. Davis,³ K. De Bruyn,⁶ S. De Capua,⁵⁶ M. De Cian,¹² J. M. De Miranda,¹ L. De Paula,² M. De Serio,^{14,l} P. De Simone,¹⁹ C. T. Dean,⁵³ D. Decamp,⁴ M. Deckenhoff,¹⁰ L. Del Buono,⁸ M. Demmer,¹⁰ A. Dendek,²⁸ D. Derkach,³⁵ O. Deschamps,⁵ F. Dettori,⁴ B. Dey,²² A. Di Canto,⁴⁰ H. Dijkstra,⁴⁰ F. Dordei,⁴⁰ M. Dorigo,⁴¹ A. Dosil Suárez,³⁹ A. Dovbnya,⁴⁵ K. Dreimanis,⁵⁴ L. Dufour,⁴³ G. Dujany,⁵⁶ K. Dungs,⁴⁰ P. Durante,⁴⁰ R. Dzhelyadin,³⁷ A. Dziurda,⁴⁰ A. Dzyuba,³¹ N. Déleage,⁴ S. Easo,⁵¹ M. Ebert,⁵² U. Egede,⁵⁵ V. Egorychev,³² S. Eidelman,^{36,e} S. Eisenhardt,⁵² U. Eitschberger,¹⁰ R. Ekelhof,¹⁰ L. Eklund,⁵³ S. Ely,⁶¹ S. Esen,¹² H. M. Evans,⁴⁹ T. Evans,⁵⁷ A. Falabella,¹⁵ N. Farley,⁴⁷ S. Farry,⁵⁴ R. Fay,⁵⁴ D. Fazzini,^{21,c} D. Ferguson,⁵² A. Fernandez Prieto,³⁹ F. Ferrari,^{15,40} F. Ferreira Rodrigues,² M. Ferro-Luzzi,⁴⁰ S. Filippov,³⁴ R. A. Fini,¹⁴ M. Fiore,^{17,a} M. Fiorini,^{17,a} M. Firlej,²⁸ C. Fitzpatrick,⁴¹ T. Fiutowski,²⁸ F. Fleuret,^{7,m} K. Fohl,⁴⁰ M. Fontana,^{16,40} F. Fontanelli,^{20,i} D. C. Forshaw,⁶¹ R. Forty,⁴⁰ V. Franco Lima,⁵⁴ M. Frank,⁴⁰ C. Frei,⁴⁰ J. Fu,^{22,n} W. Funk,⁴⁰ E. Furfaro,^{25,h} C. Färber,⁴⁰ A. Gallas Torreira,³⁹ D. Galli,^{15,g} S. Gallorini,²³ S. Gambetta,⁵² M. Gandelman,² P. Gandini,⁵⁷ Y. Gao,³ L. M. Garcia Martin,⁶⁹ J. García Pardiñas,³⁹ J. Garra Tico,⁴⁹ L. Garrido,³⁸ P. J. Garsed,⁴⁹ D. Gascon,³⁸ C. Gaspar,⁴⁰ L. Gavardi,¹⁰ G. Gazzoni,⁵ D. Gerick,¹² E. Gersabeck,¹² M. Gersabeck,⁵⁶ T. Gershon,⁵⁰ Ph. Ghez,⁴ S. Gianì,⁴¹ V. Gibson,⁴⁹ O. G. Girard,⁴¹ L. Giubega,³⁰ K. Gizdov,⁵² V. V. Gligorov,⁸ D. Golubkov,³² A. Golutvin,^{55,40} A. Gomes,^{1,o} I. V. Gorelov,³³ C. Gotti,^{21,c} E. Govorkova,⁴³ R. Graciani Diaz,³⁸ L. A. Granado Cardoso,⁴⁰ E. Graugés,³⁸ E. Graverini,⁴² G. Graziani,¹⁸ A. Greco,³⁰ R. Greim,⁹ P. Griffith,¹⁶ L. Grillo,^{21,40,c} B. R. Gruberg Cazon,⁵⁷ O. Grünberg,⁶⁷ E. Gushchin,³⁴ Yu. Guz,³⁷ T. Gys,⁴⁰ C. Göbel,⁶² T. Hadavizadeh,⁵⁷ C. Hadjivasiliou,⁵ G. Haefeli,⁴¹ C. Haen,⁴⁰ S. C. Haines,⁴⁹ B. Hamilton,⁶⁰ X. Han,¹² S. Hansmann-Menzemer,¹² N. Harnew,⁵⁷ S. T. Harnew,⁴⁸ J. Harrison,⁵⁶ M. Hatch,⁴⁰ J. He,⁶³ T. Head,⁴¹ A. Heister,⁹ K. Hennessy,⁵⁴ P. Henrard,⁵ L. Henry,⁸ E. van Herwijnen,⁴⁰ M. Heß,⁶⁷ A. Hicheur,² D. Hill,⁵⁷ C. Hombach,⁵⁶ H. Hopchev,⁴¹ W. Hulsbergen,⁴³ T. Humair,⁵⁵ M. Hushchyn,³⁵ D. Hutchcroft,⁵⁴ M. Idzik,²⁸ P. Ilten,⁵⁸ R. Jacobsson,⁴⁰ A. Jaeger,¹² J. Jalocha,⁵⁷ E. Jans,⁴³ A. Jawahery,⁶⁰ F. Jiang,³ M. John,⁵⁷ D. Johnson,⁴⁰ C. R. Jones,⁴⁹ C. Joram,⁴⁰ B. Jost,⁴⁰ N. Jurik,⁵⁷

S. Kandybei,⁴⁵ M. Karacson,⁴⁰ J. M. Kariuki,⁴⁸ S. Karodia,⁵³ M. Kecke,¹² M. Kelsey,⁶¹ M. Kenzie,⁴⁹ T. Ketel,⁴⁴ E. Khairullin,³⁵ B. Khanji,¹² C. Khurewathanakul,⁴¹ T. Kirn,⁹ S. Klaver,⁵⁶ K. Klimaszewski,²⁹ T. Klimkovich,¹¹ S. Kolliiev,⁴⁶ M. Kolpin,¹² I. Komarov,⁴¹ R. F. Koopman,⁴⁴ P. Koppenburg,⁴³ A. Kosmyntseva,³² A. Kozachuk,³³ M. Kozeiha,⁵ L. Kravchuk,³⁴ K. Kreplin,¹² M. Kreps,⁵⁰ P. Krokovny,^{36,e} F. Kruse,¹⁰ W. Krzemien,²⁹ W. Kucewicz,^{27,p} M. Kucharczyk,²⁷ V. Kudryavtsev,^{36,e} A. K. Kuonen,⁴¹ K. Kurek,²⁹ T. Kvaratskheliya,^{32,40} D. Lacarrere,⁴⁰ G. Lafferty,⁵⁶ A. Lai,¹⁶ G. Lanfranchi,¹⁹ C. Langenbruch,⁹ T. Latham,⁵⁰ C. Lazzeroni,⁴⁷ R. Le Gac,⁶ J. van Leerdam,⁴³ A. Leflat,^{33,40} J. Lefrançois,⁷ R. Lefèvre,⁵ F. Lemaitre,⁴⁰ E. Lemos Cid,³⁹ O. Leroy,⁶ T. Lesiak,²⁷ B. Leverington,¹² T. Li,³ Y. Li,⁷ T. Likhomanenko,^{35,68} R. Lindner,⁴⁰ C. Linn,⁴⁰ F. Lionetto,⁴² X. Liu,³ D. Loh,⁵⁰ I. Longstaff,⁵³ J. H. Lopes,² D. Lucchesi,^{23,q} M. Lucio Martinez,³⁹ H. Luo,⁵² A. Lupato,²³ E. Luppi,^{17,a} O. Lupton,⁴⁰ A. Lusiani,²⁴ X. Lyu,⁶³ F. Machefert,⁷ F. Maciuc,³⁰ O. Maev,³¹ K. Maguire,⁵⁶ S. Malde,⁵⁷ A. Malinin,⁶⁸ T. Maltsev,³⁶ G. Manca,^{16,k} G. Mancinelli,⁶ P. Manning,⁶¹ J. Maratas,^{5,r} J. F. Marchand,⁴ U. Marconi,¹⁵ C. Marin Benito,³⁸ M. Marinangeli,⁴¹ P. Marino,^{24,j} J. Marks,¹² G. Martellotti,²⁶ M. Martin,⁶ M. Martinelli,⁴¹ D. Martinez Santos,³⁹ F. Martinez Vidal,⁶⁹ D. Martins Tostes,² L. M. Massacrier,⁷ A. Massafferri,¹ R. Matev,⁴⁰ A. Mathad,⁵⁰ Z. Mathe,⁴⁰ C. Matteuzzi,²¹ A. Mauri,⁴² E. Maurice,^{7,m} B. Maurin,⁴¹ A. Mazurov,⁴⁷ M. McCann,^{55,40} A. McNab,⁵⁶ R. McNulty,¹³ B. Meadows,⁵⁹ F. Meier,¹⁰ M. Meissner,¹² D. Melnychuk,²⁹ M. Merk,⁴³ A. Merli,^{22,n} E. Michielin,²³ D. A. Milanes,⁶⁶ M.-N. Minard,⁴ D. S. Mitzel,¹² A. Mogini,⁸ J. Molina Rodriguez,¹ I. A. Monroy,⁶⁶ S. Monteil,⁵ M. Morandin,²³ P. Morawski,²⁸ A. Mordà,⁶ M. J. Morello,^{24,j} O. Morgunova,⁶⁸ J. Moron,²⁸ A. B. Morris,⁵² R. Mountain,⁶¹ F. Muheim,⁵² M. Mulder,⁴³ M. Mussini,¹⁵ D. Müller,⁵⁶ J. Müller,¹⁰ K. Müller,⁴² V. Müller,¹⁰ P. Naik,⁴⁸ T. Nakada,⁴¹ R. Nandakumar,⁵¹ A. Nandi,⁵⁷ I. Nasteva,² M. Needham,⁵² N. Neri,²² S. Neubert,¹² N. Neufeld,⁴⁰ M. Neuner,¹² T. D. Nguyen,⁴¹ C. Nguyen-Mau,^{41,s} S. Nieswand,⁹ R. Niet,¹⁰ N. Nikitin,³³ T. Nikodem,¹² A. Nogay,⁶⁸ A. Novoselov,³⁷ D. P. O'Hanlon,⁵⁰ A. Oblakowska-Mucha,²⁸ V. Obraztsov,³⁷ S. Ogilvy,¹⁹ R. Oldeman,^{16,k} C. J. G. Onderwater,⁷⁰ J. M. Otalora Goicochea,² A. Otto,⁴⁰ P. Owen,⁴² A. Oyanguren,⁶⁹ P. R. Pais,⁴¹ A. Palano,^{14,l} M. Palutan,¹⁹ A. Papanestis,⁵¹ M. Pappagallo,^{14,l} L. L. Pappalardo,^{17,a} W. Parker,⁶⁰ C. Parkes,⁵⁶ G. Passaleva,¹⁸ A. Pastore,^{14,l} G. D. Patel,⁵⁴ M. Patel,⁵⁵ C. Patrignani,^{15,g} A. Pearce,⁴⁰ A. Pellegrino,⁴³ G. Penso,²⁶ M. Pepe Altarelli,⁴⁰ S. Perazzini,⁴⁰ P. Perret,⁵ L. Pescatore,⁴¹ K. Petridis,⁴⁸ A. Petrolini,^{20,i} A. Petrov,⁶⁸ M. Petruzzo,^{22,n} E. Picatoste Olloqui,³⁸ B. Pietrzyk,⁴ M. Pikies,²⁷ D. Pinci,²⁶ A. Pistone,²⁰ A. Piucci,¹² V. Placinta,³⁰ S. Playfer,⁵² M. Plo Casasus,³⁹ T. Poikela,⁴⁰ F. Polci,⁸ A. Poluektov,^{50,36} I. Polyakov,⁶¹ E. Polycarpo,² G. J. Pomery,⁴⁸ A. Popov,³⁷ D. Popov,^{11,40} B. Popovici,³⁰ S. Poslavskii,³⁷ C. Potterat,² E. Price,⁴⁸ J. D. Price,⁵⁴ J. Prisciandaro,^{39,40} A. Pritchard,⁵⁴ C. Prouve,⁴⁸ V. Pugatch,⁴⁶ A. Puig Navarro,⁴² G. Punzi,^{24,t} W. Qian,⁵⁰ R. Quagliani,^{7,48} B. Rachwal,²⁷ J. H. Rademacker,⁴⁸ M. Rama,²⁴ M. Ramos Pernas,³⁹ M. S. Rangel,² I. Raniuk,⁴⁵ F. Ratnikov,³⁵ G. Raven,⁴⁴ F. Redi,⁵⁵ S. Reichert,¹⁰ A. C. dos Reis,¹ C. Remon Alepuz,⁶⁹ V. Renaudin,⁷ S. Ricciardi,⁵¹ S. Richards,⁴⁸ M. Rihl,⁴⁰ K. Rinnert,⁵⁴ V. Rives Molina,³⁸ P. Robbe,^{7,40} A. B. Rodrigues,¹ E. Rodrigues,⁵⁹ J. A. Rodriguez Lopez,⁶⁶ P. Rodriguez Perez,⁵⁶ A. Rogozhnikov,³⁵ S. Roiser,⁴⁰ A. Rollings,⁵⁷ V. Romanovskiy,³⁷ A. Romero Vidal,³⁹ J. W. Ronayne,¹³ M. Rotondo,¹⁹ M. S. Rudolph,⁶¹ T. Ruf,⁴⁰ P. Ruiz Valls,⁶⁹ J. J. Saborido Silva,³⁹ E. Sadykhov,³² N. Sagidova,³¹ B. Saitta,^{16,k} V. Salustino Guimaraes,¹ C. Sanchez Mayordomo,⁶⁹ B. Sanmartin Sedes,³⁹ R. Santacesaria,²⁶ C. Santamarina Rios,³⁹ M. Santimaria,¹⁹ E. Santovetti,^{25,h} A. Sarti,^{19,u} C. Satriano,^{26,v} A. Satta,²⁵ D. M. Saunders,⁴⁸ D. Savrina,^{32,33} S. Schael,⁹ M. Schellenberg,¹⁰ M. Schiller,⁵³ H. Schindler,⁴⁰ M. Schlupp,¹⁰ M. Schmelling,¹¹ T. Schmelzer,¹⁰ B. Schmidt,⁴⁰ O. Schneider,⁴¹ A. Schopper,⁴⁰ H. F. Schreiner,⁵⁹ K. Schubert,¹⁰ M. Schubiger,⁴¹ M.-H. Schune,⁷ R. Schwemmer,⁴⁰ B. Sciascia,¹⁹ A. Sciubba,^{26,u} A. Semennikov,³² A. Sergi,⁴⁷ N. Serra,⁴² J. Serrano,⁶ L. Sestini,²³ P. Seyfert,²¹ M. Shapkin,³⁷ I. Shapoval,⁴⁵ Y. Shcheglov,³¹ T. Shears,⁵⁴ L. Shekhtman,^{36,e} V. Shevchenko,⁶⁸ B. G. Siddi,^{17,40} R. Silva Coutinho,⁴² L. Silva de Oliveira,² G. Simi,^{23,q} S. Simone,^{14,l} M. Sirendi,⁴⁹ N. Skidmore,⁴⁸ T. Skwarnicki,⁶¹ E. Smith,⁵⁵ I. T. Smith,⁵² J. Smith,⁴⁹ M. Smith,⁵⁵ H. Snoek,⁴³ I. Soares Lavra,¹ M. D. Sokoloff,⁵⁹ F. J. P. Soler,⁵³ B. Souza De Paula,² B. Spaan,¹⁰ P. Spradlin,⁵³ S. Sridharan,⁴⁰ F. Stagni,⁴⁰ M. Stahl,¹² S. Stahl,⁴⁰ P. Stefko,⁴¹ S. Stefkova,⁵⁵ O. Steinkamp,⁴² S. Stemmler,¹² O. Stenyakin,³⁷ H. Stevens,¹⁰ S. Stevenson,⁵⁷ S. Stoica,³⁰ S. Stone,⁶¹ B. Storaci,⁴² S. Stracka,^{24,t} M. E. Stramaglia,⁴¹ M. Straticiu,³⁰ U. Straumann,⁴² L. Sun,⁶⁴ W. Sutcliffe,⁵⁵ K. Swientek,²⁸ V. Syropoulos,⁴⁴ M. Szczekowski,²⁹ T. Szumlak,²⁸ S. T'Jampens,⁴ A. Tayduganov,⁶ T. Tekampe,¹⁰ G. Tellarini,^{17,a} F. Teubert,⁴⁰ E. Thomas,⁴⁰ J. van Tilburg,⁴³ M. J. Tilley,⁵⁵ V. Tisserand,⁴ M. Tobin,⁴¹ S. Tolck,⁴⁹ L. Tomassetti,^{17,a} D. Tonelli,⁴⁰ S. Topp-Joergensen,⁵⁷ F. Toriello,⁶¹ E. Tournefier,⁴ S. Tourneur,⁴¹ K. Trabelsi,⁴¹ M. Traill,⁵³ M. T. Tran,⁴¹ M. Tresch,⁴² A. Trisovic,⁴⁰ A. Tsaregorodtsev,⁶ P. Tsopelas,⁴³ A. Tully,⁴⁹ N. Tuning,⁴³ A. Ukleja,²⁹ A. Ustyuzhanin,³⁵ U. Uwer,¹² C. Vacca,^{16,k} V. Vagnoni,^{15,40} A. Valassi,⁴⁰ S. Valat,⁴⁰ G. Valenti,¹⁵ R. Vazquez Gomez,¹⁹ P. Vazquez Regueiro,³⁹ S. Vecchi,¹⁷ M. van Veghel,⁴³ J. J. Velthuis,⁴⁸ M. Veltri,^{18,w} G. Veneziano,⁵⁷ A. Venkateswaran,⁶¹

M. Vernet,⁵ M. Vesterinen,¹² J. V. Viana Barbosa,⁴⁰ B. Viaud,⁷ D. Vieira,⁶³ M. Vieites Diaz,³⁹ H. Viemann,⁶⁷ X. Vilasis-Cardona,^{38,f} M. Vitti,⁴⁹ V. Volkov,³³ A. Vollhardt,⁴² B. Voneki,⁴⁰ A. Vorobyev,³¹ V. Vorobyev,^{36,e} C. Voß,⁹ J. A. de Vries,⁴³ C. Vázquez Sierra,³⁹ R. Waldi,⁶⁷ C. Wallace,⁵⁰ R. Wallace,¹³ J. Walsh,²⁴ J. Wang,⁶¹ D. R. Ward,⁴⁹ H. M. Wark,⁵⁴ N. K. Watson,⁴⁷ D. Websdale,⁵⁵ A. Weiden,⁴² M. Whitehead,⁴⁰ J. Wicht,⁵⁰ G. Wilkinson,^{57,40} M. Wilkinson,⁶¹ M. Williams,⁴⁰ M. P. Williams,⁴⁷ M. Williams,⁵⁸ T. Williams,⁴⁷ F. F. Wilson,⁵¹ J. Wimberley,⁶⁰ J. Wishahi,¹⁰ W. Wislicki,²⁹ M. Witek,²⁷ G. Wormser,⁷ S. A. Wotton,⁴⁹ K. Wraight,⁵³ K. Wyllie,⁴⁰ Y. Xie,⁶⁵ Z. Xing,⁶¹ Z. Xu,⁴ Z. Yang,³ Y. Yao,⁶¹ H. Yin,⁶⁵ J. Yu,⁶⁵ X. Yuan,^{36,e} O. Yushchenko,³⁷ K. A. Zarebski,⁴⁷ M. Zavertyaev,^{11,b} L. Zhang,³ Y. Zhang,⁷ A. Zhelezov,¹² Y. Zheng,⁶³ X. Zhu,³ V. Zhukov,³³ and S. Zucchelli¹⁵

(LHCb Collaboration)

- ¹Centro Brasileiro de Pesquisas Físicas (CBPF), Rio de Janeiro, Brazil
²Universidade Federal do Rio de Janeiro (UFRJ), Rio de Janeiro, Brazil
³Center for High Energy Physics, Tsinghua University, Beijing, China
⁴LAPP, Université Savoie Mont-Blanc, CNRS/IN2P3, Annecy-Le-Vieux, France
⁵Clermont Université, Université Blaise Pascal, CNRS/IN2P3, LPC, Clermont-Ferrand, France
⁶CPPM, Aix-Marseille Université, CNRS/IN2P3, Marseille, France
⁷LAL, Université Paris-Sud, CNRS/IN2P3, Orsay, France
⁸LPNHE, Université Pierre et Marie Curie, Université Paris Diderot, CNRS/IN2P3, Paris, France
⁹I. Physikalisches Institut, RWTH Aachen University, Aachen, Germany
¹⁰Fakultät Physik, Technische Universität Dortmund, Dortmund, Germany
¹¹Max-Planck-Institut für Kernphysik (MPIK), Heidelberg, Germany
¹²Physikalisches Institut, Ruprecht-Karls-Universität Heidelberg, Heidelberg, Germany
¹³School of Physics, University College Dublin, Dublin, Ireland
¹⁴Sezione INFN di Bari, Bari, Italy
¹⁵Sezione INFN di Bologna, Bologna, Italy
¹⁶Sezione INFN di Cagliari, Cagliari, Italy
¹⁷Sezione INFN di Ferrara, Ferrara, Italy
¹⁸Sezione INFN di Firenze, Firenze, Italy
¹⁹Laboratori Nazionali dell'INFN di Frascati, Frascati, Italy
²⁰Sezione INFN di Genova, Genova, Italy
²¹Sezione INFN di Milano Bicocca, Milano, Italy
²²Sezione INFN di Milano, Milano, Italy
²³Sezione INFN di Padova, Padova, Italy
²⁴Sezione INFN di Pisa, Pisa, Italy
²⁵Sezione INFN di Roma Tor Vergata, Roma, Italy
²⁶Sezione INFN di Roma La Sapienza, Roma, Italy
²⁷Henryk Niewodniczanski Institute of Nuclear Physics Polish Academy of Sciences, Kraków, Poland
²⁸AGH - University of Science and Technology, Faculty of Physics and Applied Computer Science, Kraków, Poland
²⁹National Center for Nuclear Research (NCBJ), Warsaw, Poland
³⁰Horia Hulubei National Institute of Physics and Nuclear Engineering, Bucharest-Magurele, Romania
³¹Petersburg Nuclear Physics Institute (PNPI), Gatchina, Russia
³²Institute of Theoretical and Experimental Physics (ITEP), Moscow, Russia
³³Institute of Nuclear Physics, Moscow State University (SINP MSU), Moscow, Russia
³⁴Institute for Nuclear Research of the Russian Academy of Sciences (INR RAN), Moscow, Russia
³⁵Yandex School of Data Analysis, Moscow, Russia
³⁶Budker Institute of Nuclear Physics (SB RAS), Novosibirsk, Russia
³⁷Institute for High Energy Physics (IHEP), Protvino, Russia
³⁸ICCUB, Universitat de Barcelona, Barcelona, Spain
³⁹Universidad de Santiago de Compostela, Santiago de Compostela, Spain
⁴⁰European Organization for Nuclear Research (CERN), Geneva, Switzerland
⁴¹Institute of Physics, Ecole Polytechnique Fédérale de Lausanne (EPFL), Lausanne, Switzerland
⁴²Physik-Institut, Universität Zürich, Zürich, Switzerland
⁴³Nikhef National Institute for Subatomic Physics, Amsterdam, Netherlands
⁴⁴Nikhef National Institute for Subatomic Physics and VU University Amsterdam, Amsterdam, Netherlands
⁴⁵NSC Kharkiv Institute of Physics and Technology (NSC KIPT), Kharkiv, Ukraine
⁴⁶Institute for Nuclear Research of the National Academy of Sciences (KINR), Kyiv, Ukraine

- ⁴⁷*University of Birmingham, Birmingham, United Kingdom*
- ⁴⁸*H.H. Wills Physics Laboratory, University of Bristol, Bristol, United Kingdom*
- ⁴⁹*Cavendish Laboratory, University of Cambridge, Cambridge, United Kingdom*
- ⁵⁰*Department of Physics, University of Warwick, Coventry, United Kingdom*
- ⁵¹*STFC Rutherford Appleton Laboratory, Didcot, United Kingdom*
- ⁵²*School of Physics and Astronomy, University of Edinburgh, Edinburgh, United Kingdom*
- ⁵³*School of Physics and Astronomy, University of Glasgow, Glasgow, United Kingdom*
- ⁵⁴*Oliver Lodge Laboratory, University of Liverpool, Liverpool, United Kingdom*
- ⁵⁵*Imperial College London, London, United Kingdom*
- ⁵⁶*School of Physics and Astronomy, University of Manchester, Manchester, United Kingdom*
- ⁵⁷*Department of Physics, University of Oxford, Oxford, United Kingdom*
- ⁵⁸*Massachusetts Institute of Technology, Cambridge, Massachusetts, USA*
- ⁵⁹*University of Cincinnati, Cincinnati, Ohio, USA*
- ⁶⁰*University of Maryland, College Park, Maryland, USA*
- ⁶¹*Syracuse University, Syracuse, New York, USA*
- ⁶²*Pontifícia Universidade Católica do Rio de Janeiro (PUC-Rio), Rio de Janeiro, Brazil*
(associated with *Institution Universidade Federal do Rio de Janeiro (UFRJ), Rio de Janeiro, Brazil*)
- ⁶³*University of Chinese Academy of Sciences, Beijing, China*
(associated with *Institution Center for High Energy Physics, Tsinghua University, Beijing, China*)
- ⁶⁴*School of Physics and Technology, Wuhan University, Wuhan, China*
(associated with *Institution Center for High Energy Physics, Tsinghua University, Beijing, China*)
- ⁶⁵*Institute of Particle Physics, Central China Normal University, Wuhan, Hubei, China*
(associated with *Institution Center for High Energy Physics, Tsinghua University, Beijing, China*)
- ⁶⁶*Departamento de Física, Universidad Nacional de Colombia, Bogota, Colombia*
(associated with *Institution LPNHE, Université Pierre et Marie Curie, Université Paris Diderot, CNRS/IN2P3, Paris, France*)
- ⁶⁷*Institut für Physik, Universität Rostock, Rostock, Germany*
(associated with *Institution Physikalisches Institut, Ruprecht-Karls-Universität Heidelberg, Heidelberg, Germany*)
- ⁶⁸*National Research Centre Kurchatov Institute, Moscow, Russia*
(associated with *Institution Institute of Theoretical and Experimental Physics (ITEP), Moscow, Russia*)
- ⁶⁹*Instituto de Física Corpuscular, Centro Mixto Universidad de Valencia - CSIC, Valencia, Spain*
(associated with *Institution CCUB, Universitat de Barcelona, Barcelona, Spain*)
- ⁷⁰*Van Swinderen Institute, University of Groningen, Groningen, Netherlands*
(associated with *Institution Nikhef National Institute for Subatomic Physics, Amsterdam, Netherlands*)

^aAlso at Università di Ferrara, Ferrara, Italy.

^bAlso at P.N. Lebedev Physical Institute, Russian Academy of Science (LPI RAS), Moscow, Russia.

^cAlso at Università di Milano Bicocca, Milano, Italy.

^dAlso at Università di Modena e Reggio Emilia, Modena, Italy.

^eAlso at Novosibirsk State University, Novosibirsk, Russia.

^fAlso at LIFAELS, La Salle, Universitat Ramon Llull, Barcelona, Spain.

^gAlso at Università di Bologna, Bologna, Italy.

^hAlso at Università di Roma Tor Vergata, Roma, Italy.

ⁱAlso at Università di Genova, Genova, Italy.

^jAlso at Scuola Normale Superiore, Pisa, Italy.

^kAlso at Università di Cagliari, Cagliari, Italy.

^lAlso at Università di Bari, Bari, Italy.

^mAlso at Laboratoire Leprince-Ringuet, Palaiseau, France.

ⁿAlso at Università degli Studi di Milano, Milano, Italy.

^oAlso at Universidade Federal do Triângulo Mineiro (UFTM), Uberaba-MG, Brazil.

^pAlso at AGH - University of Science and Technology, Faculty of Computer Science, Electronics and Telecommunications, Kraków, Poland.

^qAlso at Università di Padova, Padova, Italy.

^rAlso at Iligan Institute of Technology (IIT), Iligan, Philippines.

^sAlso at Hanoi University of Science, Hanoi, Viet Nam.

^tAlso at Università di Pisa, Pisa, Italy.

^uAlso at Università di Roma La Sapienza, Roma, Italy.

^vAlso at Università della Basilicata, Potenza, Italy.

^wAlso at Università di Urbino, Urbino, Italy.